

Received 3 May 2018
Accepted 8 May 2018

Edited by W. T. A. Harrison, University of Aberdeen, Scotland

‡ Additional correspondence author, e-mail: omarsa@usm.my.

Keywords: crystal structure; ruthenium; cluster; carbonyl; Hirshfeld surface analysis.

CCDC reference: 1842044

Supporting information: this article has supporting information at journals.iucr.org/e

Undecacarbonyl[(4-methylsulfanylphenyl)diphenylphosphane]triruthenium(0): crystal structure and Hirshfeld surface analysis

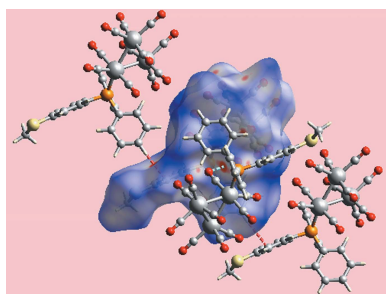
Omar bin Shawkataly,^a‡ Hafiz Malik Hussien Abdelnasir,^b Siti Syaida Sirat,^a Mukesh M. Jotani^c and Edward R. T. Tieckink^d*

^aChemical Sciences Programme, School of Distance Education, Universiti Sains Malaysia, 11800 USM, Penang, Malaysia, ^bDepartment of Chemistry, Alzaiem Alazhari University, 1933, Khartoum, Sudan, ^cDepartment of Physics, Bhavan's Sheth R. A. College of Science, Ahmedabad, Gujarat 380001, India, and ^dResearch Centre for Crystalline Materials, School of Science and Technology, Sunway University, 47500 Bandar Sunway, Selangor Darul Ehsan, Malaysia. *Correspondence e-mail: edwardt@sunway.edu.my

The title cluster compound, $[\text{Ru}_3(\text{C}_{19}\text{H}_{17}\text{PS})(\text{CO})_{11}]$, comprises a triangle of Ru^0 atoms, two of which are bonded to four carbonyl ligands. The third metal atom is bound to three carbonyl ligands and the phosphane-P atom of a dissymmetric phosphane ligand, $\text{PPh}_2(\text{C}_6\text{H}_4\text{SMe}-4)$; no $\text{Ru}\cdots\text{S}$ interactions are observed. The phosphane occupies an equatorial position and its proximity to an $\text{Ru}-\text{Ru}$ edge results in the elongation of this bond with respect to the others [2.8933 (2) Å *cf.* 2.8575 (2) and 2.8594 (3) Å]. In the crystal, phenyl-C—H···O(carbonyl) and carbonyl-O···O(carbonyl) [2.817 (2) Å] interactions combine to form a supramolecular chain propagating along [111]; the chains pack without directional interactions between them. The carbonyl-O···O(carbonyl) and other weak contacts have an influence upon the Hirshfeld surfaces with O···H contacts making the greatest contribution, *i.e.* 37.4% *cf.* 15.8% for O···O and 15.6% for H···H contacts.

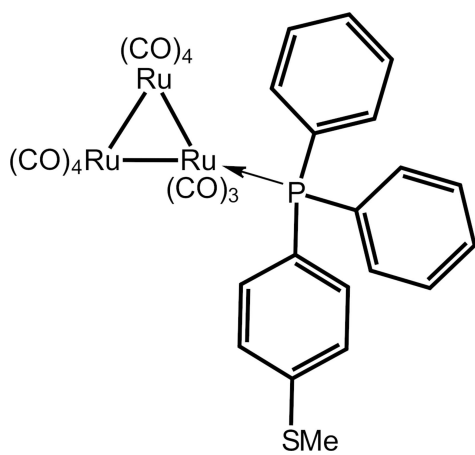
1. Chemical context

Tertiary phosphanes (PR_3) have played a major role in the formation and subsequent chemistry of metal carbonyl clusters, often relating to the promising catalytic activity of the products (Bruce *et al.*, 2005; Shawkataly *et al.*, 2013; Park *et al.*, 2016). In general, the thermal reaction of $\text{Ru}_3(\text{CO})_{12}$ with PR_3 leads to $\text{Ru}_3(\text{CO})_{12-n}(\text{PR}_3)_n$, $n = 1-4$, cluster compounds (Bruce *et al.*, 1988, 1989). The steric and electronic effects of PR_3 often results in the lengthening of $\text{Ru}-\text{Ru}$ bonds in the Ru_3 triangle as compared with the parent compound, $\text{Ru}_3(\text{CO})_{12}$, thereby making the cluster more reactive (Bruce *et al.*, 1989). The $\text{PPh}_2\text{C}_6\text{H}_4\text{SMe}$ ligand is of interest because it contains two different potential donor groups, *i.e.* P and S, which can result in variable substitution patterns. For example, in the $\text{Cu}_{22}\text{Se}_6(\text{SePh})_{10}[\text{PPh}_2(\text{C}_6\text{H}_4\text{SMe})_8]$ cluster, only the P atom of the $\text{PPh}_2\text{C}_6\text{H}_4\text{SMe}$ ligand is coordinated to the metal centre while the thiomethyl group remains uncoordinated (Fuhr *et al.*, 2002). However, the thiomethyl group can further react with other metal atoms to provide opportunities in surface chemistry (Fuhr *et al.*, 2002). The known crystal structures of triruthenium clusters with the $\text{PPh}_2(\text{C}_6\text{H}_4\text{SMe})$ ligand are surprisingly few in number (Shawkataly *et al.*, 2011*a,b*). Herein, the crystal and molecular structures of the title compound, $\text{Ru}_3(\text{CO})_{11}\text{PPh}_2(\text{C}_6\text{H}_4\text{SMe}-4)$ (I), are



OPEN ACCESS

described as well as an analysis of the calculated Hirshfeld surface.



2. Structural commentary

The molecular structure of $\text{Ru}_3(\text{CO})_{11}\text{PPh}_2(\text{C}_6\text{H}_4\text{SMe}-4)$, (I), is shown in Fig. 1. The molecule comprises an Ru_3 triangle with one Ru centre being bound, equatorially, by the phosphane ligand. The Ru–Ru bond lengths in the Ru_3 triangle are not equivalent with the Ru1–Ru2 bond of 2.8933 (2) Å being longer than the Ru1–Ru3 and Ru2–Ru3 bonds of 2.8575 (2) and 2.8594 (3) Å, respectively. This disparity probably reflects the steric hindrance exerted by the phosphane ligand which occupies the region in the vicinity of the Ru1–Ru2 bond. Some general trends in the geometric parameters involving the carbonyl ligands may be discerned, the relatively high errors in some of the parameters notwithstanding. Thus, the Ru–C bond distances involving carbonyl groups lying in the plane of the Ru_3 ring are generally shorter than those occupying positions perpendicular to the plane, with the respective ranges in Ru–C bond lengths being 1.897 (3)–

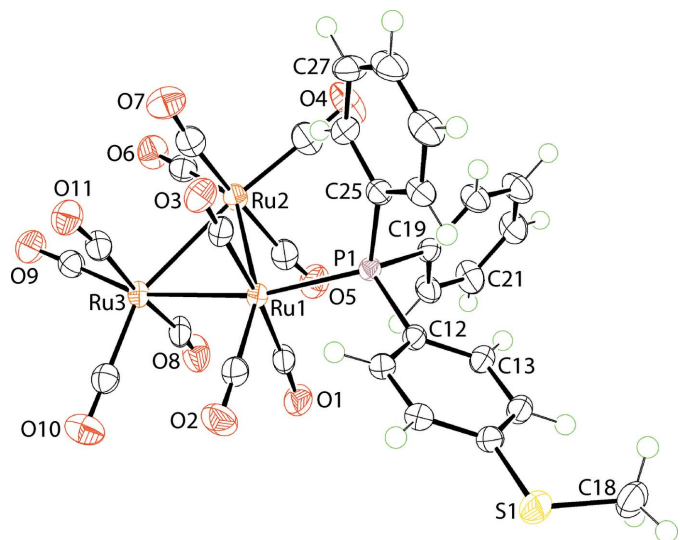


Figure 1

The molecular structure of (I) showing the atom-labelling scheme and displacement ellipsoids at the 70% probability level.

1.930 (3) Å and 1.937 (2)–1.953 (3) Å. While the Ru–C≡O angles are all close to linear, two distinctive ranges in angles are evident. The Ru–C≡O angles involving carbonyl groups lying in the plane of the Ru_3 ring lie in the range 177.3 (2)–178.7 (2)° while the range for the perpendicularly orientated carbonyl groups is 172.1 (2)–174.6 (2)°. The trend for longer Ru–C distances and greater deviations from linearity of the Ru–C≡O angles for the axial carbonyl ligands, which occupy positions *trans* to other carbonyl ligands, is consistent with some semi-bridging character for these carbonyl ligands. Thus, the closest intramolecular Ru···C(carbonyl) contact of 3.233 (3) Å is formed by the C8-carbonyl ligand which exhibits the maximum deviation from linearity, *i.e.* 172.1 (2)°.

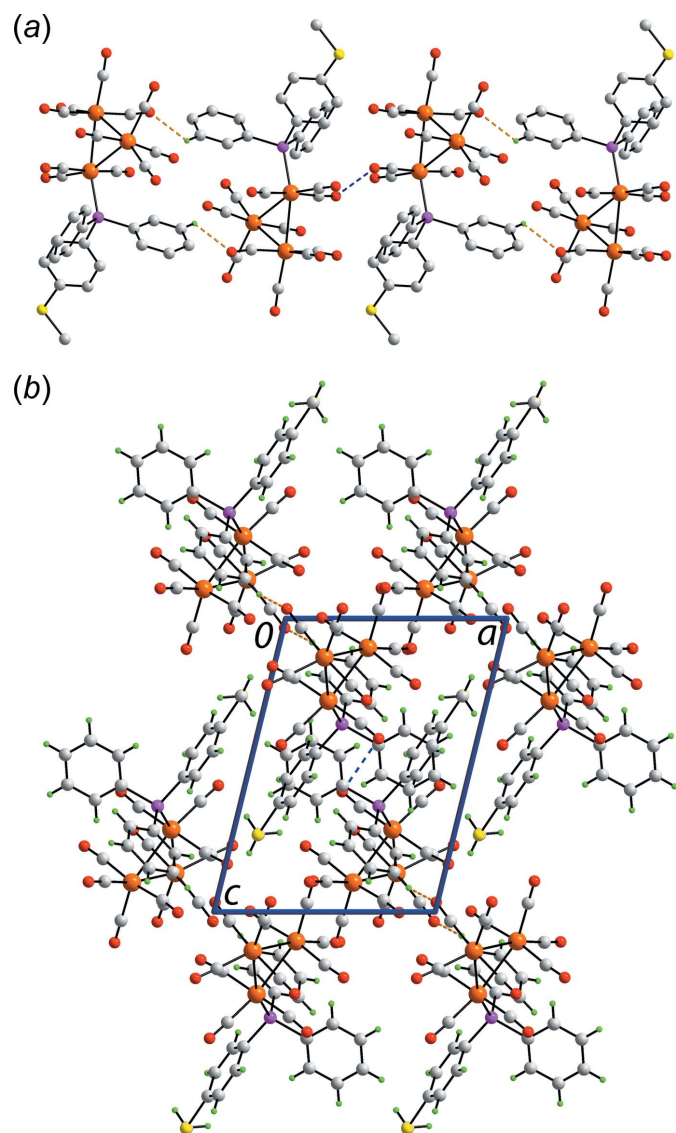


Figure 2

Molecular packing in (I): (a) The supramolecular chain sustained by C–H···O and O···O interactions and (b) a view of the unit-cell contents shown in projection down the *b* axis. The C–H···O and O···O interactions are shown as orange and blue dashed lines, respectively.

Table 1
Hydrogen-bond geometry (\AA , $^\circ$).

$D-\text{H}\cdots A$	$D-\text{H}$	$\text{H}\cdots A$	$D\cdots A$	$D-\text{H}\cdots A$
C21—H21 \cdots O8 ⁱ	0.95	2.55	3.238 (3)	129

Symmetry code: (i) $-x, -y, -z$.

3. Supramolecular features

The molecular packing of (I) features phenyl-C—H \cdots O(carbonyl) interactions occurring about a centre of inversion and leading to centrosymmetric dimers, Table 1. Connections between the dimers leading to a supramolecular chain along [111] are of the type carbonyl-O \cdots O(carbonyl), Fig. 2a. The O3 \cdots O3ⁱ separation is 2.817 (2) \AA , a distance less than the sum of the van der Waals radii of oxygen, *i.e.* 3.04 \AA (Bondi, 1964); symmetry operation (i): $1 - x, 1 - y, 1 - z$. Such intermolecular O \cdots O interactions are examples of homoatomic chalcogen bonding which are rarest for the smaller oxygen atoms (Gleiter *et al.*, 2018). The chains pack without directional interactions between them according to the criteria assumed in PLATON (Spek, 2009). A view of the unit-cell contents is shown in Fig. 2b.

4. Analysis of the Hirshfeld surface

The Hirshfeld surface calculations of (I) were performed in accordance with a recent publication on a related ruthenium cluster compound (Shawkataly *et al.*, 2017). Two views of the Hirshfeld surface mapped over d_{norm} are shown in Fig. 3. A spot near the O8 atom in Fig. 3a, results from the C21—H \cdots O8 interaction (Table 1). The presence of a diminutive red spot near the carbonyl-O3 atom in Fig. 3b reflects the significance of the short O3 \cdots O3 contact mentioned in *Supramolecular features*. The intense red spots near the methylsulfanylbenzene-C16 and phenyl-H28 atoms indicate the significance of this short interatomic C \cdots H/H \cdots C contact (Table 2; calculated in CrystalExplorer3.1 (Wolff *et al.*, 2012)). In addition, interactions involving several carbonyl groups results in short O \cdots O and C \cdots O/O \cdots C contacts (Table 2) and are characterized as faint red spots in Fig. 3. The Hirshfeld surfaces mapped over the electrostatic potential illustrated in Fig. 4 also reflect the involvement of different atoms in the

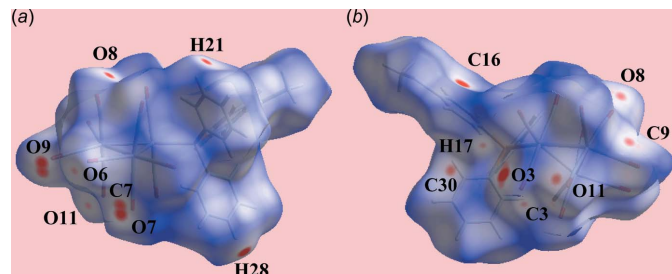


Figure 3
Two views of the Hirshfeld surface of (I) mapped over d_{norm} in the range -0.106 to $+1.524$ au.

Table 2
Summary of short interatomic contacts (\AA) in (I).

Contact	Distance	Symmetry operation
O3 \cdots O3	2.817 (2)	$1 - x, 1 - y, 1 - z$
O6 \cdots O11	2.986 (3)	$1 - x, 1 - y, -z$
C3 \cdots O3	3.150 (3)	$1 - x, 1 - y, 1 - z$
C7 \cdots O9	3.088 (3)	$1 - x, 1 - y, -z$
C9 \cdots O8	3.137 (3)	$-x, 1 - y, -z$
C17 \cdots O11	3.196 (3)	$1 - x, 1 - y, 1 - z$
C30 \cdots O11	3.122 (3)	$1 - x, 1 - y, 1 - z$
C16 \cdots H28	2.59	$-1 + x, y, z$
O3 \cdots H17	2.54	$1 - x, 1 - y, 1 - z$
H18B \cdots H20	2.44	$-x, -y, 1 - z$

intermolecular interactions through the appearance of blue and red regions around the participating atoms, and correspond to positive and negative electrostatic potential, respectively. As highlighted in Fig. 4a, an intramolecular carbonyl-C4≡O4 \cdots Cg(C19—C24) contact is evident. Carbonyl \cdots π (arene) interactions are known to be important in the structural chemistry of metal carbonyls (Zukerman-Schpector *et al.*, 2011). Here, the O4 \cdots Cg(C19—C24) separation is 3.850 (3) \AA and the angle subtended at the O4 atom is 90.1 (2) $^\circ$, indicating a side-on (parallel) approach between the residues. The environment about a reference molecule, showing short interatomic O \cdots O and C \cdots H/H \cdots C contacts significant in the molecule packing of (I), is illustrated in Fig. 5.

The overall two-dimensional fingerprint plot for (I) and those delineated into H \cdots H, O \cdots H/H \cdots O, O \cdots O, C \cdots H/H \cdots C and C \cdots O/O \cdots C contacts (McKinnon *et al.*, 2007) are illustrated in Fig. 6; the percentage contributions from the different interatomic contacts to the Hirshfeld surfaces are summarized in Table 3. In the fingerprint plot delineated into H \cdots H contacts, the relatively small, *i.e.* 15.6%, contribution from these contacts to the Hirshfeld surfaces is due to the presence of the carbonyl groups on the Ru-cluster which leads to an increase in the contribution of O \cdots H/H \cdots O contacts to the Hirshfeld surface, *i.e.* 37.4%. The single tip at $d_e + d_i \sim 2.4$ \AA in the H \cdots H delineated fingerprint plot, which has a broad appearance, arises from a van der Waals contact between the methyl-H18B and phenyl-H20 atoms (Table 2). The two pairs of adjacent peaks at $d_e + d_i \sim 2.5$ and 2.6 \AA in the fingerprint plot delineated into O \cdots H/H \cdots O contacts are the

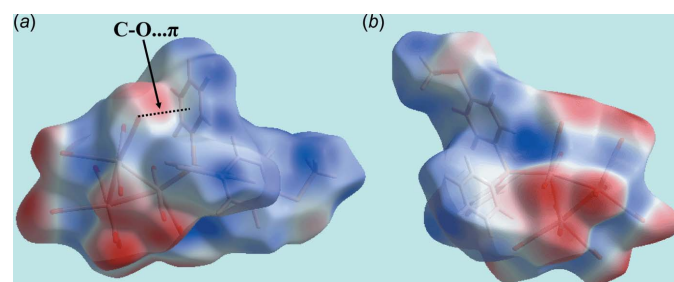


Figure 4

Two views of the Hirshfeld surface of (I) mapped over the electrostatic potential in the range ± 0.046 au. The red and blue regions represent negative and positive electrostatic potentials, respectively.

Table 3

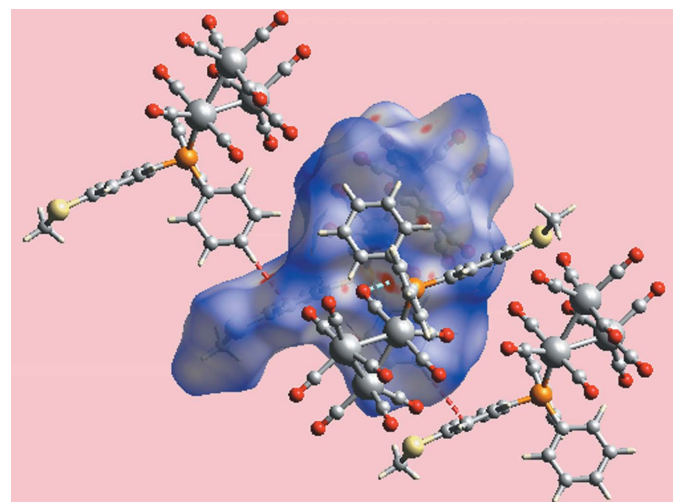
Percentage contributions of interatomic contacts to the Hirshfeld surface for (I).

Contact	Percentage contribution
H···H	15.6
O···H/H···O	37.4
C···H/H···C	14.7
O···O	15.8
C···O/O···C	9.0
S···H/H···S	2.6
S···O/O···S	2.4
C···C	1.6
C···S/S···C	0.9

result of the interatomic C—H···O interaction discussed above (Table 1) and a short interatomic O···H/H···O contact (Table 2), respectively. The influence of the significant interatomic O3···O3 contact (Fig. 5) and other such short interatomic contacts (Table 3) are viewed as the distribution of points with the rocket-like tip extending from $d_e + d_i \sim 2.8$ Å in the plot delineated into O···O contacts. In the fingerprint plot delineated into C···O/O···C contacts, the short interatomic contacts between carbonyl-C7 and -O9 atoms appear as the pair of thin tips at $d_e + d_i \sim 3.1$ Å superimposed on the parabolic distribution of points characterizing other such short interatomic contacts through the points around $d_e = d_i = 1.6$ Å. The other dominant short interatomic C···H/H···C contacts (Table 2) result in the pair of forceps-like tips at $d_e + d_i \sim 2.6$ Å in the respective delineated fingerprint plot. The small contribution from other remaining interatomic contacts summarized in Table 3 have negligible effect on the packing.

5. Database survey

As mentioned in the *Chemical context*, there are two other Ru₃ clusters in the literature having the same (4-methyl-

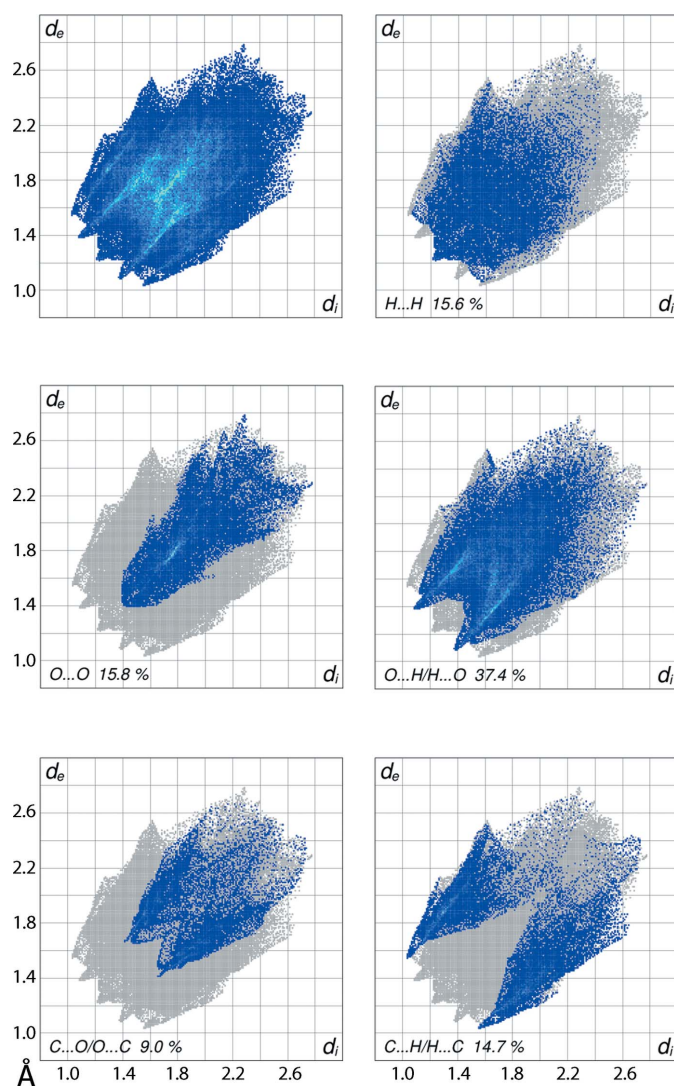
**Figure 5**

A view of the Hirshfeld surface of (I) mapped over d_{norm} in the range -0.090 to $+1.204$ au highlighting O···O and C···H/H···C contacts by sky-blue and red dashed lines, respectively.

sulfanylphenyl)diphenylphosphane ligand as in (I). These are formulated as Ru₃(CO)₉PPh₂(C₆H₄SM₄-4)(Ph₂PCH₂PPh₂) (II) (Shawkataly *et al.*, 2011b) and its arsenic analogue, Ru₃(CO)₉PPh₂(C₆H₄SM₄-4)(Ph₂AsCH₂AsPh₂) (Shawkataly *et al.*, 2011a), in each of which the bidentate ligand bridges the other two ruthenium atoms in the triangle. The structural motif found in (I), *i.e.* with an equatorially substituted phosphane ligand, is consistent with the approximately 35 literature precedents with the general formula Ru₃(CO)₁₁PRR'R'' and several examples where the phosphane ligand is bidentate bridging, *i.e.* Ru₃(CO)₁₁PR(R')-R''-(R')RPRu₃(CO)₁₁ (Groom *et al.*, 2016). There are no crystallographic examples with perpendicular mono-substitution of phosphane ligands in Ru₃(CO)₁₁PRR'R''.

6. Synthesis and crystallization

All reactions were carried out under an inert atmosphere of oxygen-free nitrogen (OFN) using standard Schlenk techni-

**Figure 6**

The full two-dimensional fingerprint plot for (I) and those delineated into H···H, O···H/H···O, O···O, C···H/H···C and C···O/O···C contacts.

ques. $\text{Ru}_3(\text{CO})_{12}$ was purchased from Aldrich and $\text{PPh}_2\text{C}_6\text{H}_4\text{SMe}$ was synthesized as reported previously (Fuhr *et al.*, 2002). $\text{Ru}_3(\text{CO})_{11}\text{P}(\text{C}_6\text{H}_4\text{SMe}-4)\text{Ph}_2$ (**I**) was synthesized by dissolving $\text{Ru}_3(\text{CO})_{12}$ (100 mg, 0.0015 mmol) and $\text{PPh}_2(\text{C}_6\text{H}_4\text{SMe})$ (48 mg, 0.0015 mmol) in tetrahydrofuran (25 ml). The reaction mixture was treated dropwise with sodium diphenylketyl solution until the colour of the mixture turned from orange to dark red and then stirred for 30 min. The solvent was evaporated under vacuum and the residue was chromatographed by preparative TLC. Elution with 7:3 *n*-hexane/dichloromethane mixture gave four bands and the major orange fraction was characterized as (**I**) (117 mg, 79.6%). Orange crystals were crystallized from solvent diffusion of dichloromethane into a methanol solution of (**I**). Analysis calculated for $\text{C}_{30}\text{H}_{17}\text{O}_{11}\text{PRu}_3\text{S}$: C, 39.18; H, 1.86%. Found: C, 39.60; H, 1.90%. IR (C_6H_{12}): $\nu(\text{CO})$ 2097(*m*), 2059(*w*), 2046(*m*), 2015(*s*), 1989(*w*) cm^{-1} . ^1H NMR (CDCl_3): δ 7.45–7.23 (*m*, 14H, Ph, C_6H_4), 2.48 (*s*, Me). ^{13}C NMR (CDCl_3): δ 204.24 (Ru—CO), 135.19–125.37 (Ph), 14.79 (Me). ^{31}P NMR (CDCl_3): δ 34.28 (*s*).

7. Refinement

Crystal data, data collection and structure refinement details are summarized in Table 4. The carbon-bound H atoms were placed in calculated positions ($\text{C}-\text{H} = 0.95\text{--}0.98 \text{\AA}$) and were included in the refinement in the riding-model approximation, with $U_{\text{iso}}(\text{H})$ set to $1.2\text{--}1.5U_{\text{eq}}(\text{C})$. Owing to poor agreement, four reflections, *i.e.* (1 7 14), (10 2 6), (3 12 12) and (6 16 10), were omitted from the final cycles of refinement. The maximum and minimum residual electron density peaks of 1.97 and 0.98 e \AA^{-3} , respectively, were located 0.69 and 0.61 \AA from the atoms Ru1 and Ru3, respectively.

Funding information

OBS wishes to thank Universiti Sains Malaysia (USM) for Research University Grant No. 1001/PJJAUH/8011002. SSS thanks the Universiti Teknologi Mara (UiTM) for a PhD scholarship.

References

Table 4 Experimental details.	
Crystal data	
Chemical formula	$[\text{Ru}_3(\text{C}_{19}\text{H}_{17}\text{PS})(\text{CO})_{11}]$
M_r	919.67
Crystal system, space group	Triclinic, $P\bar{1}$
Temperature (K)	100
$a, b, c (\text{\AA})$	9.6922 (1), 12.7459 (2), 13.6030 (2)
$\alpha, \beta, \gamma (^{\circ})$	103.301 (1), 102.938 (1), 91.771 (1)
$V (\text{\AA}^3)$	1587.83 (4)
Z	2
Radiation type	Mo $K\alpha$
$\mu (\text{mm}^{-1})$	1.58
Crystal size (mm)	0.32 \times 0.30 \times 0.14
Data collection	
Diffractometer	Bruker SMART APEXII CCD
Absorption correction	Multi-scan (SADABS; Bruker, 2009)
T_{\min}, T_{\max}	0.448, 0.526
No. of measured, independent and observed [$I > 2\sigma(I)$] reflections	56976, 15652, 11725
R_{int}	0.042
(sin θ/λ) _{max} (\AA^{-1})	0.842
Refinement	
$R[F^2 > 2\sigma(F^2)], wR(F^2), S$	0.041, 0.097, 1.03
No. of reflections	15652
No. of parameters	416
H-atom treatment	H-atom parameters constrained
$\Delta\rho_{\text{max}}, \Delta\rho_{\text{min}} (\text{e } \text{\AA}^{-3})$	1.97, -0.98
Computer programs:	
<i>APEX2</i> and <i>SAINT</i> (Bruker, 2009), <i>SHELXS</i> (Sheldrick, 2008), <i>SHELXL2014</i> (Sheldrick, 2015), <i>ORTEP-3 for Windows</i> (Farrugia, 2012), <i>DIAMOND</i> (Brandenburg, 2006) and <i>publCIF</i> (Westrip, 2010).	
Farrugia, L. J. (2012). <i>J. Appl. Cryst.</i> 45 , 849–854.	
Fuhr, O., Meredith, A. & Fenske, D. (2002). <i>J. Chem. Soc. Dalton Trans.</i> pp. 4091–4094.	
Gleiter, R., Haberhauer, G., Werz, D. B., Rominger, F. & Bleiholder, C. (2018). <i>Chem. Rev.</i> 118 , 2010–2041.	
Groom, C. R., Bruno, I. J., Lightfoot, M. P. & Ward, S. C. (2016). <i>Acta Cryst. B</i> 72 , 171–179.	
McKinnon, J. J., Jayatilaka, D. & Spackman, M. A. (2007). <i>Chem. Commun.</i> pp. 3814–3816.	
Park, B. Y., Luong, T., Sato, H. & Krische, M. J. (2016). <i>J. Org. Chem.</i> 81 , 8585–8594.	
Shawkataly, O. bin, Khan, I. A., Hafiz Malik, H. A., Yeap, C. S. & Fun, H.-K. (2011a). <i>Acta Cryst. E</i> 67 , m179–m180.	
Shawkataly, O. bin, Khan, I. A., Hafiz Malik, H. A., Yeap, C. S. & Fun, H.-K. (2011b). <i>Acta Cryst. E</i> 67 , m218–m219.	
Shawkataly, O. bin, Sirat, S. S., Jotani, M. M. & Tiekink, E. R. T. (2017). <i>Acta Cryst. E</i> 73 , 1652–1657.	
Shawkataly, O. B., Sirat, S. S., Khan, I. A. & Fun, H. K. (2013). <i>Polyhedron</i> , 63 , 173–181.	
Sheldrick, G. M. (2008). <i>Acta Cryst. A</i> 64 , 112–122.	
Sheldrick, G. M. (2015). <i>Acta Cryst. C</i> 71 , 3–8.	
Spek, A. L. (2009). <i>Acta Cryst. D</i> 65 , 148–155.	
Westrip, S. P. (2010). <i>J. Appl. Cryst.</i> 43 , 920–925.	
Wolff, S. K., Grimwood, D. J., McKinnon, J. J., Turner, M. J., Jayatilaka, D. & Spackman, M. A. (2012). <i>CrystalExplorer</i> . The University of Western Australia.	
Zukerman-Schpector, J., Haiduc, I. & Tiekink, E. R. T. (2011). <i>Chem. Commun.</i> 47 , 12682–12684.	

supporting information

Acta Cryst. (2018). E74, 791–795 [https://doi.org/10.1107/S2056989018006989]

Undecacarbonyl[(4-methylsulfanylphenyl)diphenylphosphane]triruthenium(0): crystal structure and Hirshfeld surface analysis

Omar bin Shawkataly, Hafiz Malik Hussien Abdelnasir, Siti Syaida Sirat, Mukesh M. Jotani and Edward R. T. Tieckink

Computing details

Data collection: *APEX2* (Bruker, 2009); cell refinement: *SAINT* (Bruker, 2009); data reduction: *SAINT* (Bruker, 2009); program(s) used to solve structure: *SHELXS* (Sheldrick, 2008); program(s) used to refine structure: *SHELXL2014* (Sheldrick, 2015); molecular graphics: *ORTEP-3 for Windows* (Farrugia, 2012) and *DIAMOND* (Brandenburg, 2006); software used to prepare material for publication: *publCIF* (Westrip, 2010).

Undecacarbonyl[(4-methylsulfanylphenyl)diphenylphosphane]triruthenium(0)

Crystal data

[Ru₃(C₁₉H₁₇PS)(CO)₁₁]

$M_r = 919.67$

Triclinic, $P\bar{1}$

$a = 9.6922$ (1) Å

$b = 12.7459$ (2) Å

$c = 13.6030$ (2) Å

$\alpha = 103.301$ (1)°

$\beta = 102.938$ (1)°

$\gamma = 91.771$ (1)°

$V = 1587.83$ (4) Å³

$Z = 2$

$F(000) = 896$

$D_x = 1.924$ Mg m⁻³

Mo $K\alpha$ radiation, $\lambda = 0.71073$ Å

Cell parameters from 9414 reflections

$\theta = 2.6\text{--}36.5$ °

$\mu = 1.58$ mm⁻¹

$T = 100$ K

Block, orange

0.32 × 0.30 × 0.14 mm

Data collection

Bruker SMART APEXII CCD
diffractometer

Radiation source: fine-focus sealed tube

φ and ω scans

Absorption correction: multi-scan
(*SADABS*; Bruker, 2009)

$T_{\min} = 0.448$, $T_{\max} = 0.526$

56976 measured reflections

15652 independent reflections

11725 reflections with $I > 2\sigma(I)$

$R_{\text{int}} = 0.042$

$\theta_{\max} = 36.8$ °, $\theta_{\min} = 2.0$ °

$h = -16 \rightarrow 16$

$k = -21 \rightarrow 21$

$l = -22 \rightarrow 22$

Refinement

Refinement on F^2

Least-squares matrix: full

$R[F^2 > 2\sigma(F^2)] = 0.041$

$wR(F^2) = 0.097$

$S = 1.03$

15652 reflections

416 parameters

0 restraints

Primary atom site location: structure-invariant
direct methods

Hydrogen site location: inferred from
neighbouring sites

H-atom parameters constrained

$w = 1/[\sigma^2(F_o^2) + (0.048P)^2]$
where $P = (F_o^2 + 2F_c^2)/3$

$(\Delta/\sigma)_{\max} = 0.001$

$\Delta\rho_{\max} = 1.97 \text{ e } \text{\AA}^{-3}$ $\Delta\rho_{\min} = -0.98 \text{ e } \text{\AA}^{-3}$ *Special details*

Geometry. All esds (except the esd in the dihedral angle between two l.s. planes) are estimated using the full covariance matrix. The cell esds are taken into account individually in the estimation of esds in distances, angles and torsion angles; correlations between esds in cell parameters are only used when they are defined by crystal symmetry. An approximate (isotropic) treatment of cell esds is used for estimating esds involving l.s. planes.

Fractional atomic coordinates and isotropic or equivalent isotropic displacement parameters (\AA^2)

	<i>x</i>	<i>y</i>	<i>z</i>	$U_{\text{iso}}^*/U_{\text{eq}}$
Ru1	0.28387 (2)	0.33186 (2)	0.28051 (2)	0.01428 (4)
Ru2	0.40348 (2)	0.29273 (2)	0.09996 (2)	0.01862 (4)
Ru3	0.21842 (2)	0.46106 (2)	0.13284 (2)	0.01626 (4)
S1	0.11319 (7)	0.13142 (5)	0.73844 (5)	0.02529 (12)
P1	0.37139 (6)	0.19229 (4)	0.36008 (4)	0.01376 (10)
O1	-0.00653 (19)	0.21034 (14)	0.16345 (15)	0.0282 (4)
O2	0.1200 (2)	0.45096 (15)	0.43099 (15)	0.0308 (4)
O3	0.55312 (18)	0.47646 (14)	0.40979 (13)	0.0251 (4)
O4	0.6007 (3)	0.11066 (18)	0.10236 (18)	0.0435 (5)
O5	0.1625 (2)	0.11127 (15)	-0.00206 (15)	0.0312 (4)
O6	0.4152 (2)	0.34976 (16)	-0.10467 (15)	0.0309 (4)
O7	0.6584 (2)	0.45662 (17)	0.22391 (15)	0.0319 (4)
O8	-0.0055 (2)	0.29918 (15)	-0.03258 (16)	0.0326 (4)
O9	0.2453 (2)	0.57908 (15)	-0.03402 (14)	0.0288 (4)
O10	-0.0099 (2)	0.57899 (17)	0.22667 (16)	0.0335 (4)
O11	0.4558 (2)	0.62755 (14)	0.27933 (14)	0.0273 (4)
C1	0.1048 (3)	0.25236 (18)	0.20139 (19)	0.0207 (4)
C2	0.1833 (3)	0.40534 (19)	0.37650 (19)	0.0215 (4)
C3	0.4559 (3)	0.42297 (18)	0.35766 (18)	0.0195 (4)
C4	0.5271 (3)	0.1777 (2)	0.1037 (2)	0.0279 (5)
C5	0.2456 (3)	0.1817 (2)	0.03905 (19)	0.0246 (5)
C6	0.4106 (3)	0.3274 (2)	-0.0295 (2)	0.0236 (5)
C7	0.5600 (3)	0.4000 (2)	0.18099 (19)	0.0238 (5)
C8	0.0801 (3)	0.35306 (19)	0.03187 (19)	0.0228 (5)
C9	0.2348 (3)	0.53252 (19)	0.02662 (18)	0.0211 (4)
C10	0.0760 (3)	0.53550 (19)	0.19383 (19)	0.0223 (4)
C11	0.3718 (3)	0.56093 (19)	0.22852 (19)	0.0215 (4)
C12	0.2835 (2)	0.16989 (17)	0.45989 (17)	0.0155 (4)
C13	0.2366 (2)	0.06656 (18)	0.46472 (17)	0.0174 (4)
H13	0.2421	0.0056	0.4108	0.021*
C14	0.1818 (2)	0.05201 (18)	0.54780 (18)	0.0189 (4)
H14	0.1480	-0.0183	0.5491	0.023*
C15	0.1765 (2)	0.14016 (18)	0.62855 (17)	0.0179 (4)
C16	0.2236 (2)	0.24400 (18)	0.62442 (17)	0.0176 (4)
H16	0.2203	0.3048	0.6792	0.021*
C17	0.2748 (2)	0.25804 (17)	0.54035 (17)	0.0166 (4)
H17	0.3045	0.3288	0.5376	0.020*
C18	0.1152 (3)	-0.0110 (2)	0.7356 (2)	0.0276 (5)

H18A	0.0428	-0.0525	0.6756	0.041*
H18B	0.0949	-0.0232	0.7997	0.041*
H18C	0.2090	-0.0346	0.7299	0.041*
C19	0.3634 (2)	0.05642 (16)	0.27629 (16)	0.0153 (4)
C20	0.2408 (2)	0.01554 (18)	0.19821 (19)	0.0216 (4)
H20	0.1635	0.0592	0.1886	0.026*
C21	0.2302 (3)	-0.08793 (19)	0.1345 (2)	0.0268 (5)
H21	0.1462	-0.1145	0.0818	0.032*
C22	0.3416 (3)	-0.15220 (19)	0.1476 (2)	0.0253 (5)
H22	0.3348	-0.2228	0.1037	0.030*
C23	0.4638 (3)	-0.1130 (2)	0.2255 (2)	0.0264 (5)
H23	0.5405	-0.1572	0.2350	0.032*
C24	0.4747 (2)	-0.00928 (18)	0.28960 (19)	0.0214 (4)
H24	0.5585	0.0168	0.3427	0.026*
C25	0.5593 (2)	0.21583 (17)	0.43099 (17)	0.0171 (4)
C26	0.6609 (3)	0.24650 (19)	0.3821 (2)	0.0224 (4)
H26	0.6323	0.2535	0.3126	0.027*
C27	0.8033 (3)	0.2669 (2)	0.4343 (2)	0.0282 (5)
H27	0.8715	0.2876	0.4003	0.034*
C28	0.8460 (3)	0.2571 (2)	0.5359 (2)	0.0288 (5)
H28	0.9431	0.2725	0.5721	0.035*
C29	0.7475 (3)	0.2249 (2)	0.5841 (2)	0.0266 (5)
H29	0.7772	0.2172	0.6533	0.032*
C30	0.6042 (2)	0.20356 (18)	0.53226 (18)	0.0195 (4)
H30	0.5371	0.1806	0.5660	0.023*

Atomic displacement parameters (\AA^2)

	U^{11}	U^{22}	U^{33}	U^{12}	U^{13}	U^{23}
Ru1	0.01599 (8)	0.01239 (7)	0.01479 (7)	0.00070 (5)	0.00376 (6)	0.00392 (6)
Ru2	0.02282 (9)	0.01803 (8)	0.01699 (8)	0.00456 (7)	0.00739 (7)	0.00527 (6)
Ru3	0.01832 (8)	0.01340 (7)	0.01637 (8)	0.00103 (6)	0.00223 (6)	0.00411 (6)
S1	0.0303 (3)	0.0269 (3)	0.0244 (3)	0.0041 (2)	0.0138 (2)	0.0103 (2)
P1	0.0135 (2)	0.0127 (2)	0.0147 (2)	0.00001 (18)	0.00275 (18)	0.00325 (18)
O1	0.0219 (9)	0.0246 (9)	0.0366 (10)	-0.0025 (7)	0.0012 (8)	0.0107 (8)
O2	0.0334 (10)	0.0308 (10)	0.0317 (10)	0.0124 (8)	0.0161 (8)	0.0052 (8)
O3	0.0263 (9)	0.0226 (8)	0.0236 (9)	-0.0045 (7)	0.0038 (7)	0.0031 (7)
O4	0.0515 (14)	0.0407 (12)	0.0419 (12)	0.0280 (11)	0.0132 (11)	0.0125 (10)
O5	0.0386 (11)	0.0241 (9)	0.0308 (10)	-0.0003 (8)	0.0110 (8)	0.0042 (8)
O6	0.0403 (11)	0.0320 (10)	0.0250 (9)	0.0068 (8)	0.0130 (8)	0.0103 (8)
O7	0.0289 (10)	0.0379 (11)	0.0280 (10)	-0.0020 (8)	0.0092 (8)	0.0046 (8)
O8	0.0327 (10)	0.0215 (9)	0.0355 (10)	-0.0014 (7)	-0.0062 (8)	0.0053 (8)
O9	0.0333 (10)	0.0297 (9)	0.0255 (9)	0.0008 (8)	0.0080 (8)	0.0103 (8)
O10	0.0272 (10)	0.0376 (11)	0.0334 (10)	0.0080 (8)	0.0092 (8)	0.0014 (9)
O11	0.0287 (9)	0.0231 (8)	0.0266 (9)	-0.0030 (7)	0.0032 (7)	0.0032 (7)
C1	0.0237 (11)	0.0159 (9)	0.0239 (11)	0.0033 (8)	0.0049 (9)	0.0080 (8)
C2	0.0216 (11)	0.0206 (10)	0.0238 (11)	0.0024 (8)	0.0051 (9)	0.0087 (9)
C3	0.0240 (11)	0.0162 (9)	0.0196 (10)	0.0013 (8)	0.0064 (8)	0.0059 (8)

C4	0.0329 (14)	0.0297 (13)	0.0233 (12)	0.0088 (11)	0.0091 (10)	0.0081 (10)
C5	0.0319 (13)	0.0226 (11)	0.0215 (11)	0.0054 (10)	0.0099 (10)	0.0060 (9)
C6	0.0249 (12)	0.0235 (11)	0.0237 (11)	0.0037 (9)	0.0092 (9)	0.0051 (9)
C7	0.0284 (12)	0.0250 (11)	0.0203 (10)	0.0060 (9)	0.0094 (9)	0.0061 (9)
C8	0.0252 (12)	0.0165 (10)	0.0257 (11)	0.0008 (8)	0.0013 (9)	0.0081 (9)
C9	0.0211 (11)	0.0197 (10)	0.0212 (10)	0.0018 (8)	0.0038 (8)	0.0033 (8)
C10	0.0222 (11)	0.0212 (10)	0.0219 (11)	-0.0004 (9)	0.0024 (9)	0.0054 (9)
C11	0.0227 (11)	0.0185 (10)	0.0227 (11)	0.0024 (8)	0.0035 (9)	0.0057 (8)
C12	0.0141 (9)	0.0159 (9)	0.0166 (9)	0.0008 (7)	0.0019 (7)	0.0061 (7)
C13	0.0177 (10)	0.0168 (9)	0.0175 (9)	-0.0010 (7)	0.0031 (8)	0.0054 (8)
C14	0.0183 (10)	0.0183 (10)	0.0210 (10)	-0.0005 (8)	0.0039 (8)	0.0075 (8)
C15	0.0154 (10)	0.0205 (10)	0.0197 (10)	0.0025 (8)	0.0050 (8)	0.0079 (8)
C16	0.0163 (10)	0.0185 (9)	0.0180 (9)	0.0022 (8)	0.0044 (8)	0.0039 (8)
C17	0.0151 (9)	0.0167 (9)	0.0183 (9)	0.0012 (7)	0.0038 (7)	0.0050 (8)
C18	0.0314 (13)	0.0298 (13)	0.0268 (12)	0.0003 (10)	0.0104 (10)	0.0143 (10)
C19	0.0157 (9)	0.0127 (8)	0.0167 (9)	-0.0003 (7)	0.0041 (7)	0.0023 (7)
C20	0.0174 (10)	0.0169 (10)	0.0276 (11)	0.0012 (8)	-0.0001 (9)	0.0047 (9)
C21	0.0240 (12)	0.0170 (10)	0.0305 (13)	-0.0020 (9)	-0.0058 (10)	0.0002 (9)
C22	0.0298 (13)	0.0149 (10)	0.0262 (12)	0.0010 (9)	0.0040 (10)	-0.0022 (9)
C23	0.0249 (12)	0.0192 (11)	0.0315 (13)	0.0068 (9)	0.0044 (10)	0.0005 (9)
C24	0.0182 (10)	0.0195 (10)	0.0223 (10)	0.0028 (8)	-0.0002 (8)	0.0012 (8)
C25	0.0146 (9)	0.0146 (9)	0.0200 (10)	0.0002 (7)	0.0018 (8)	0.0024 (8)
C26	0.0195 (11)	0.0222 (11)	0.0271 (11)	0.0001 (8)	0.0064 (9)	0.0087 (9)
C27	0.0156 (11)	0.0257 (12)	0.0424 (15)	-0.0003 (9)	0.0072 (10)	0.0063 (11)
C28	0.0152 (11)	0.0236 (11)	0.0397 (15)	0.0009 (9)	-0.0024 (10)	0.0006 (11)
C29	0.0243 (12)	0.0238 (11)	0.0244 (11)	0.0048 (9)	-0.0031 (9)	-0.0003 (9)
C30	0.0174 (10)	0.0177 (9)	0.0203 (10)	0.0032 (8)	0.0014 (8)	0.0015 (8)

Geometric parameters (\AA , $\text{^{\circ}}$)

Ru1—C2	1.897 (3)	C13—C14	1.397 (3)
Ru1—C1	1.937 (2)	C13—H13	0.9500
Ru1—C3	1.941 (2)	C14—C15	1.390 (3)
Ru1—P1	2.3714 (5)	C14—H14	0.9500
Ru1—Ru3	2.8575 (2)	C15—C16	1.404 (3)
Ru1—Ru2	2.8933 (2)	C16—C17	1.389 (3)
Ru2—C4	1.924 (3)	C16—H16	0.9500
Ru2—C6	1.927 (2)	C17—H17	0.9500
Ru2—C5	1.946 (3)	C18—H18A	0.9800
Ru2—C7	1.953 (3)	C18—H18B	0.9800
Ru2—Ru3	2.8594 (3)	C18—H18C	0.9800
Ru3—C9	1.908 (2)	C19—C24	1.392 (3)
Ru3—C10	1.930 (3)	C19—C20	1.398 (3)
Ru3—C8	1.942 (2)	C20—C21	1.388 (3)
Ru3—C11	1.944 (2)	C20—H20	0.9500
S1—C15	1.763 (2)	C21—C22	1.380 (4)
S1—C18	1.808 (3)	C21—H21	0.9500
P1—C12	1.826 (2)	C22—C23	1.390 (4)

P1—C19	1.830 (2)	C22—H22	0.9500
P1—C25	1.840 (2)	C23—C24	1.393 (3)
O1—C1	1.142 (3)	C23—H23	0.9500
O2—C2	1.136 (3)	C24—H24	0.9500
O3—C3	1.138 (3)	C25—C30	1.395 (3)
O4—C4	1.130 (3)	C25—C26	1.397 (3)
O5—C5	1.136 (3)	C26—C27	1.389 (3)
O6—C6	1.133 (3)	C26—H26	0.9500
O7—C7	1.134 (3)	C27—C28	1.387 (4)
O8—C8	1.136 (3)	C27—H27	0.9500
O9—C9	1.141 (3)	C28—C29	1.375 (4)
O10—C10	1.132 (3)	C28—H28	0.9500
O11—C11	1.139 (3)	C29—C30	1.397 (3)
C12—C17	1.396 (3)	C29—H29	0.9500
C12—C13	1.401 (3)	C30—H30	0.9500
C2—Ru1—C1	87.40 (10)	O11—C11—Ru3	172.7 (2)
C2—Ru1—C3	90.22 (10)	C17—C12—C13	118.4 (2)
C1—Ru1—C3	174.97 (9)	C17—C12—P1	118.62 (15)
C2—Ru1—P1	101.13 (7)	C13—C12—P1	122.67 (17)
C1—Ru1—P1	95.84 (6)	C14—C13—C12	120.9 (2)
C3—Ru1—P1	88.97 (7)	C14—C13—H13	119.6
C2—Ru1—Ru3	97.52 (7)	C12—C13—H13	119.6
C1—Ru1—Ru3	83.06 (6)	C15—C14—C13	120.2 (2)
C3—Ru1—Ru3	92.87 (6)	C15—C14—H14	119.9
P1—Ru1—Ru3	161.254 (16)	C13—C14—H14	119.9
C2—Ru1—Ru2	156.94 (7)	C14—C15—C16	119.3 (2)
C1—Ru1—Ru2	92.30 (7)	C14—C15—S1	124.25 (17)
C3—Ru1—Ru2	88.15 (7)	C16—C15—S1	116.43 (17)
P1—Ru1—Ru2	101.829 (15)	C17—C16—C15	120.1 (2)
Ru3—Ru1—Ru2	59.628 (6)	C17—C16—H16	119.9
C4—Ru2—C6	102.37 (11)	C15—C16—H16	119.9
C4—Ru2—C5	87.57 (11)	C16—C17—C12	121.1 (2)
C6—Ru2—C5	95.01 (10)	C16—C17—H17	119.4
C4—Ru2—C7	91.05 (11)	C12—C17—H17	119.5
C6—Ru2—C7	93.55 (10)	S1—C18—H18A	109.5
C5—Ru2—C7	171.43 (10)	S1—C18—H18B	109.5
C4—Ru2—Ru3	169.28 (8)	H18A—C18—H18B	109.5
C6—Ru2—Ru3	88.28 (7)	S1—C18—H18C	109.5
C5—Ru2—Ru3	92.72 (7)	H18A—C18—H18C	109.5
C7—Ru2—Ru3	87.07 (7)	H18B—C18—H18C	109.5
C4—Ru2—Ru1	109.84 (8)	C24—C19—C20	118.6 (2)
C6—Ru2—Ru1	147.73 (7)	C24—C19—P1	121.93 (17)
C5—Ru2—Ru1	84.63 (7)	C20—C19—P1	119.49 (17)
C7—Ru2—Ru1	87.89 (7)	C21—C20—C19	121.0 (2)
Ru3—Ru2—Ru1	59.563 (6)	C21—C20—H20	119.5
C9—Ru3—C10	103.41 (10)	C19—C20—H20	119.5
C9—Ru3—C8	89.88 (10)	C22—C21—C20	120.1 (2)

C10—Ru3—C8	93.49 (10)	C22—C21—H21	119.9
C9—Ru3—C11	89.20 (10)	C20—C21—H21	119.9
C10—Ru3—C11	92.35 (10)	C21—C22—C23	119.6 (2)
C8—Ru3—C11	174.14 (10)	C21—C22—H22	120.2
C9—Ru3—Ru1	160.67 (7)	C23—C22—H22	120.2
C10—Ru3—Ru1	95.01 (7)	C22—C23—C24	120.4 (2)
C8—Ru3—Ru1	94.86 (7)	C22—C23—H23	119.8
C11—Ru3—Ru1	84.18 (7)	C24—C23—H23	119.8
C9—Ru3—Ru2	101.48 (7)	C23—C24—C19	120.3 (2)
C10—Ru3—Ru2	154.74 (7)	C23—C24—H24	119.8
C8—Ru3—Ru2	82.25 (7)	C19—C24—H24	119.8
C11—Ru3—Ru2	92.26 (7)	C30—C25—C26	118.7 (2)
Ru1—Ru3—Ru2	60.808 (6)	C30—C25—P1	122.05 (17)
C15—S1—C18	102.86 (11)	C26—C25—P1	119.26 (17)
C12—P1—C19	103.17 (10)	C27—C26—C25	120.7 (2)
C12—P1—C25	102.11 (10)	C27—C26—H26	119.7
C19—P1—C25	102.31 (10)	C25—C26—H26	119.7
C12—P1—Ru1	114.43 (7)	C28—C27—C26	120.1 (2)
C19—P1—Ru1	117.78 (7)	C28—C27—H27	120.0
C25—P1—Ru1	114.99 (7)	C26—C27—H27	120.0
O1—C1—Ru1	172.8 (2)	C29—C28—C27	119.8 (2)
O2—C2—Ru1	177.3 (2)	C29—C28—H28	120.1
O3—C3—Ru1	174.6 (2)	C27—C28—H28	120.1
O4—C4—Ru2	177.3 (2)	C28—C29—C30	120.7 (2)
O5—C5—Ru2	173.0 (2)	C28—C29—H29	119.7
O6—C6—Ru2	178.7 (2)	C30—C29—H29	119.7
O7—C7—Ru2	174.0 (2)	C25—C30—C29	120.1 (2)
O8—C8—Ru3	172.1 (2)	C25—C30—H30	120.0
O9—C9—Ru3	177.3 (2)	C29—C30—H30	120.0
O10—C10—Ru3	177.9 (2)		
C19—P1—C12—C17	177.86 (17)	Ru1—P1—C19—C20	-43.3 (2)
C25—P1—C12—C17	71.95 (18)	C24—C19—C20—C21	-0.6 (4)
Ru1—P1—C12—C17	-52.94 (18)	P1—C19—C20—C21	-178.9 (2)
C19—P1—C12—C13	4.2 (2)	C19—C20—C21—C22	0.0 (4)
C25—P1—C12—C13	-101.70 (19)	C20—C21—C22—C23	0.5 (4)
Ru1—P1—C12—C13	133.40 (16)	C21—C22—C23—C24	-0.4 (4)
C17—C12—C13—C14	0.3 (3)	C22—C23—C24—C19	-0.2 (4)
P1—C12—C13—C14	173.99 (17)	C20—C19—C24—C23	0.6 (4)
C12—C13—C14—C15	-1.7 (3)	P1—C19—C24—C23	178.88 (19)
C13—C14—C15—C16	1.5 (3)	C12—P1—C25—C30	6.3 (2)
C13—C14—C15—S1	-178.67 (17)	C19—P1—C25—C30	-100.32 (19)
C18—S1—C15—C14	16.8 (2)	Ru1—P1—C25—C30	130.78 (16)
C18—S1—C15—C16	-163.38 (18)	C12—P1—C25—C26	-174.03 (18)
C14—C15—C16—C17	-0.1 (3)	C19—P1—C25—C26	79.39 (19)
S1—C15—C16—C17	-179.86 (17)	Ru1—P1—C25—C26	-49.5 (2)
C15—C16—C17—C12	-1.3 (3)	C30—C25—C26—C27	-1.5 (3)
C13—C12—C17—C16	1.2 (3)	P1—C25—C26—C27	178.75 (19)

P1—C12—C17—C16	−172.74 (17)	C25—C26—C27—C28	−0.1 (4)
C12—P1—C19—C24	−94.4 (2)	C26—C27—C28—C29	1.3 (4)
C25—P1—C19—C24	11.3 (2)	C27—C28—C29—C30	−1.0 (4)
Ru1—P1—C19—C24	138.48 (17)	C26—C25—C30—C29	1.9 (3)
C12—P1—C19—C20	83.81 (19)	P1—C25—C30—C29	−178.38 (18)
C25—P1—C19—C20	−170.43 (18)	C28—C29—C30—C25	−0.7 (4)

Hydrogen-bond geometry (Å, °)

D—H···A	D—H	H···A	D···A	D—H···A
C21—H21···O8 ⁱ	0.95	2.55	3.238 (3)	129

Symmetry code: (i) $-x, -y, -z$.